

OCT 6 1948

NATIONAL ADVISORY COMMITTEE FOR AERONAUTICS

TECHNICAL NOTE

No. 1514

FATIGUE OF GUSSETED JOINTS

By Howard H. Langdon and Bernard Fried

State College of Washington



Washington

September 1948

LIBRARY COPY

APR 3 1993

LANGLEY RESEARCH CENTER
LIBRARY NASA
HAMPTON, VIRGINIA

NACA LIBRARY
LANGLEY MEMORIAL AERONAUTICAL
LABORATORY
Langley Field, Va.



NATIONAL ADVISORY COMMITTEE FOR AERONAUTICS

TECHNICAL NOTE NO. 1514

FATIGUE OF GUSSETED JOINTS

By Howard H. Langdon and Bernard Fried

SUMMARY

Fatigue tests were run on gusseted joints to determine the effect of gusset edge finish on fatigue life and to compare riveted with spot-welded assemblies. Edge finish was found to have no effect on the fatigue life of either the 24S-T or the heat-treated alloy steel (X 4130-AN-QQ-S685; yield strength, 180,000 psi) gussets tested. The riveted 24S-T joints were found to have better fatigue characteristics than the spot-welded 24S-T joints.

Additional data obtained in these tests and in a supplementing photoelastic study of the riveted-joint assembly indicated that at low load cycles stresses set up in the gusset during the riveting operation affect the fatigue life of the gusset. At high load cycles fatigue life is governed by the geometry of the gusset, that is, stress concentration at the rivet holes. Results showed that stresses introduced across the center section of the gusset by the riveting operation may reach values as high as 50 percent of the tensile stress. An improvement in gusset design is indicated on the basis of these tests.

INTRODUCTION

The objectives of this investigation were to determine the following:

1. Fatigue characteristics of riveted aluminum-alloy gussets with various edge finishes
2. Fatigue characteristics of heat-treated alloy-steel gussets
3. Fatigue strength of gusseted joints; rivets against spot welds

The loading conditions under which these tests were run were selected on the following considerations (reference 1). An airplane in level flight supports a load equivalent to 1g on the airplane. The

effect of gusts or maneuvers is to add or subtract a load increment from the load of $1g$. Hence, load cycles which were symmetrical about a given base tension load were selected.

A review of the design of gussets used on structural joints of airplanes indicated that the tensile stress on the net area of the critical section of the gusset for a load equivalent to $1g$ on the airplane was approximately 11,000 psi. Therefore, the design of the 24S-T gusset for this series of tests was such that the unit stress for the application of the base load approximates the aforementioned value.

Choice of a gusset-plate type for this series of tests was made on the same basis as would normally be made in aircraft design, that is, the type was chosen which would be most economical of material and therefore be the lightest practical construction consistent with simplicity of manufacture. The ultimate design load of 20,000 pounds for all three types of gusset was chosen to remain well within the fatigue-machine capacity and still comply with the load requirements just discussed. All supporting tubes, rivets, and mounting brackets for attaching the specimens in the testing machine were designed to be heavy enough to preclude the likelihood of failure.

The test program was expanded somewhat after the first few tests indicated the independence of fatigue strength on edge finish. Readings were taken to determine the stress distribution in the critical section of the gusset plates by use of strain gages of the SR-4 type and by photoelastic analysis.

This work was conducted at the State College of Washington under the sponsorship and with the financial assistance of the National Advisory Committee for Aeronautics.

DESCRIPTION OF APPARATUS

Fatigue Testing Machine

The fatigue testing machine with test specimen in place is shown in figure 1. The machine consists of a heavy frame anchored to a reinforced concrete base, the latter resting on rubber pads, which, in turn, rest on an isolated concrete subfloor.

At each side and within the frame are two heavy screws pinned to the upper cross frame and bolted to the steel base at the bottom. Two adjustable nuts on the lower ends of these screws are used to raise or lower the floating driving head to accommodate various-size specimens and to cushion the drop of the driving unit upon the fracture of a specimen.

The driving head is connected to the rigid outer frame by two leaf springs which offer little resistance to vertical motion of the driving head but have sufficient stiffness to prevent lateral displacement with respect to the frame. The main connection between the driving head and the frame is, of course, through the specimen. A spherical seating in the upper cross frame permits positive alinement of specimens for axial loading.

The driving mechanism consists of four cams and two shafts - two cams on each shaft. The shafts mounted in heavy ball bearings are geared to rotate in opposite directions and are driven through pulleys by a 1-horsepower induction motor. Each cam consists of an inner and an outer section; these sections are indexed and slotted so that they can be keyed to give a wide range of eccentricity to the cam. With the four cams keyed to give the same eccentricity, the synchronization is such that the centrifugal forces set up by the rotating eccentrics have a resultant in the vertical direction only.

By the use of two movable heads riding on the fixed screws of the machine proper and coupled by a worm-gear drive mechanism, two heavy calibrated coil springs can be compressed against the driving head, thus putting a base tensile load of the desired magnitude on the test specimen. The cyclic load is applied by the rotating eccentrics on the driving head. Microswitches mounted on the floating head are so arranged that the motor drive is automatically shut off when the specimen fractures or deforms excessively. The number of cycles of load reversal during a test is automatically tallied by a revolution counter. Table 1 gives data on the load cycles for the tests.

Strain Measuring Equipment

Figure 2 shows the strain measuring equipment which consists of a double-pole switching-and-driving unit equipped with special bypass switches to switch to the SR-4 static reading unit (reference 2), an RCA portable amplifier, type 319A, and a Dumont oscilloscope, type 168.

All gages had one side in common. The other side of each gage was put through the double-pole selector switch with the two common poles in parallel so as to eliminate contact resistance as far as possible. A resistance box of the plug type was used for calibrating the oscilloscope when reading dynamic strain. The driving and calibrating units are in the box shown at the left in figure 2. All circuits involved in dynamic strain measurement were shielded and grounded from the gages to the oscilloscope insofar as was possible. Mechanical strain gages of the Huggenberger and Olson Last Word types were used as checks in static tests.

TEST SPECIMENS

Table 2 provides the specifications for dimensions and materials. Also shown is the method of forming the gussets, which indicates the edge finish. No hand dressing was permitted, that is, the edges remained as stamped, saw-cut, or sheared, until tested. Inasmuch as it became evident early in the test series that edge finish had no bearing upon fatigue life of the joint, no attempt was made to record edge profile. It should be noted, however, that dies used in stamping the gussets were considered to be in the middle or latter part of their useful life and consequently the edge profiles of the stamped gussets were comparatively rough. Furthermore, specimens 11 and 13, for which the gussets were made narrow and thick relative to the initial group of specimens, were designed and saw-cut in a deliberate attempt to provide a rough edge contour and cause fatigue from the edge inward. The spot-welded specimens were fabricated completely from sheet stock, as there was an obvious difficulty in spot-welding gussets to extruded box sections or columns of the size used.

Figure 3 shows the three types of specimen tested and figure 4 shows the sections of a specimen. The 24S-T riveted gussets and columns (test specimens 1 to 10, 12, 15, 17 to 20, and 46) given in table 3 are represented by the column assembly at the left in figure 3. At the right is shown an alloy-steel heat-treated gusset riveted on 24S-T columns and given as test specimens 21 to 33 in table 3. Spot-welded Alclad 24S-T gussets and fabricated columns are shown in the center of figure 3 and given as test specimens 34 to 45 and 47 to 49 in table 3. All test specimens were factory-fabricated so as to take advantage of factory methods for uniformity of construction and of factory inspection. The end clamps are also shown in figure 3. A filler block was placed inside the column to prevent excessive distortion when tightening the clamp bolts.

TEST PROCEDURE

Table 1 gives the load cycle, the machine-applied load, the stress on the net section EE of the gusset, the stress range, the load factor, and the percentage of ultimate design load.

The matched and calibrated loading springs of the testing machine (fig. 1) were adjusted free of pressure while the end clips of the specimen were bolted to the heads of the machine. This operation lifted the lower floating head from its rubber bumpers. The spring load per tooth of the combined nut and wormwheel on the screw was determined by calibration so that, by jacking the springs the required number of teeth, the 4000-pound base load in tension was applied to the column. During this operation the upper-head spherical joint was

relaxed to a few thousandths of an inch to permit neutralization of possible machine-imposed moments on the column. The dead weight of the lower head was included in the applied load.

In order to obtain dynamic loading, the four cams on the floating head were indexed to positions consistent with rotational speed and load range in pounds, as indicated on the graph (fig. 5). The cam centrifugal forces were additive or subtractive in relation to the dead load. The errors due to inertia and momentum of the mass representing the lower head were relatively small. Actually the dynamic loading was subject to calibration, and small corrections were applied to the values shown by the graphs in figure 5.

Strain gages consistent with the SR-4 system were used in as many positions on the columns and gussets as could be applied with practical results. Gages were, as a rule, applied in similar positions on opposite sides of the column and joint. A dummy temperature-compensating gage was used in making static readings.

After setting and bolting the column, the static load was applied and verified (by strain gages on the column), the rotating cams adjusted for the dynamic load, the microswitch cut-out adjusted, and the motor started. The upper spherical joint was tightened under running condition. On coming up to speed, adjustments were made in the variable V-belt pulley as needed to obtain the desired cam speed. The dynamic strain equipment was switched on and the amplifier adjusted for oscilloscope deflection. As quickly as possible strain readings were made on all gages; following this a calibration reading was made with known resistance values bracketing the range recorded dynamically. This method of reading dynamic strain followed by calibration was done at fixed intervals, the interval depending upon the anticipated number of cycles for the applied test load. The cycle counter was read at the beginning and the end of the test.

With the oscilloscope supplied with internal horizontal sweep, the image was the familiar sine-function curve. By diminishing the internal-sweep potential to zero, the length of the resulting vertical line could be readily measured or photographed. This length was used to measure the dynamic strain. Some specimens gave warning of impending failure. A modification of the crest of the sine curve appeared as a flattening of the top, with minor crests appearing on one or both sides of the crest.

PRECISION

Column gages were used on the tubes for test programs 1 and 2 of this report wherever gusset gages were used. These column gages were used for verifying the machine-applied loads - both static and dynamic. These four column gages were read under the same conditions

and at the same time as the gusset gages. The area of the cross section of the column and the modulus of elasticity of the material were determined by related measurements and tests. This provided an independent means for checking the applied loads. When these checked within 15 percent of the predetermined loads imposed by the machine, the tests were allowed to proceed.

ANALYSIS AND DISCUSSION OF RESULTS

24S-T Riveted Gussets

Fatigue test results, with load range plotted against cycles to rupture, are shown graphically in figure 6. As is indicated in the last column of table 3, all failures started at the center of the gusset plate or at a rivet hole and progressed toward the edge. The progression of the fatigue crack is illustrated in figure 7 by specimens 5 and 8, in which the crack has started at the center but has not yet spread to the edge, and by specimen 2, in which the fracture is complete.

In an attempt to obtain a fracture starting at the edge of the gusset plate, two specimens were made in which the plate width was reduced but the thickness increased to maintain approximately the same gross and net cross-sectional areas in the gussets as in the original specimens. Although the width of these gussets was reduced 20 percent in one and 40 percent in the other, fatigue cracks still originated at the rivet holes rather than at the rough, saw-cut edges.

In addition to discounting edge finish as a factor in fatigue life, specimens 11 and 13 had significantly longer fatigue lives than the wider gusset plates under the same load conditions. (See fig. 6.) The result is attributed to the fact that these specimens had greater net areas in the region of high stress (i.e., between the rows of rivets) than the wider specimens. No effort was made to determine that shape of gusset which would give the optimum fatigue life; however, the results indicate that the thick, narrow gussets would be most favorable.

Further evidence of the low edge stresses set up in the 2.56-inch-wide gusset by the applied loads was obtained from strain-gage data on the gussets and from a photoelastic analysis of the maximum shear-stress distribution in a model of the gusset joint assembly. (See appendix.) Strain gages of the SR-4 resistance type, located approximately 1/4 inch from the gusset edge on section FF, indicated stresses between 56 and 61 percent of the average stress across that section. The photoelastic data showed that the stress at the very edge of the gusset on the same section was only 13 percent of the average stress. Since the stress at the edge of a rivet hole on section EE is 4.13

times as large (photoelastic result) as the average stress on section FF, the possibility of the influence of edge finish on fatigue life is very remote indeed.

Qualitative results showed rather early in the test program that edge finish was not a vital factor, and attention was directed toward obtaining quantitative data which might explain the occurrence of fractures across the gross section FF of the gussets at the lower load cycles. It was, of course, at once apparent that such failures were due to initial stresses across this section, presumably introduced during assembly of the joint.

Several failures of the type illustrated by specimen 9 in figure 7 occurred; the fracture occurred simultaneously across both sections EE and FF, and this observation afforded an opportunity for estimating the magnitude of these initial stresses.

With the notation

σ_{\max} maximum principal stress

σ_{\min} minimum principal stress

τ_{\max} maximum shear stress $\left(\frac{1}{2} (\sigma_{\max} - \sigma_{\min}) \right)$

it is assumed, as is generally done in design, that fatigue failure will occur under biaxial stress conditions when the maximum shear stress exceeds the shear stress of the highest stressed element of a conventional fatigue specimen at its endurance limit. Thus for cases in which failure occurs across both the gross and net sections,

$$\left(\tau_{\max} \right)_{FF} + \left(\tau'_{\max} \right)_{FF} = \left(\tau_{\max} \right)_{EE} \quad (1)$$

where

$\left(\tau_{\max} \right)_{FF}$ load-induced maximum shear stress across gross section

$\left(\tau_{\max} \right)_{EE}$ load-induced maximum shear stress across net section

$\left(\tau'_{\max} \right)_{FF}$ initial maximum shear stress across gross section

Values of $\left(\tau_{\max} \right)_{FF}$ and $\left(\tau_{\max} \right)_{EE}$ in terms of the average stress $\left(P/A \right)_{FF}$,

where P is the applied load or force and A is the area, across the gross section can be obtained directly from the photoelastic stress patterns as follows:

$$(\tau_{\max})_{FF} = \frac{1}{2} \times 1.56 (P/A)_{FF} = 0.78 (P/A)_{FF} \quad (2)$$

$$(\tau_{\max})_{EE} = \frac{1}{2} \times 4.13 (P/A)_{FF} = 2.07 (P/A)_{FF} \quad (3)$$

and equation (1) can be written

$$(\tau'_{\max})_{FF} = 1.29 (P/A)_{FF} \quad (4)$$

For failures across section FF,

$$(\tau'_{\max})_{FF} > 1.29(P/A)_{FF}$$

For failures across section EE,

$$(\tau'_{\max})_{FF} < 1.29(P/A)_{FF}$$

The value of the stress-concentration factor at the rivet hole on section EE cannot be measured with strain gages; however, strain gages could be used to check the photoelastic result for the maximum shear stress on section FF. The SR-4 gages mounted axially between rivet holes at the center of the gussets gave values of $\sigma_{\max} = 0.71(P/A)_{FF}$ statically and $\sigma_{\max} = 0.83(P/A)_{FF}$ dynamically. Gages mounted at the same point but at right angles to the direction of load gave values of $\sigma_{\min} = -0.55(P/A)_{FF}$ statically and $\sigma_{\min} = -0.62(P/A)_{FF}$ dynamically. At this point gages in these directions coincide with the directions of principal stresses and will indicate principal-stress (σ_{\max} and σ_{\min}) values.

Hence, from strain-gage data, for the static condition,

$$(\tau_{\max})_{FF} = \frac{1}{2}(\sigma_{\max} - \sigma_{\min}) = \frac{1}{2} (0.71 + 0.55)(P/A)_{FF} = 0.63(P/A)_{FF} \quad (5)$$

and for the dynamic condition,

$$(\tau_{\max})_{FF} = \frac{1}{2}(0.83 + 0.62)(P/A)_{FF} = 0.72(P/A)_{FF} \quad (6)$$

Since the photoelastic result refers to the maximum shear stress at a point and the strain gages give the shear stress over a finite area of the plate, the agreement between the two independently measured values is considered very good.

On substituting the values of $(P/A)_{FF}$ for load cycles 3 and 5 in equation (4), the initial maximum shear stress in specimens 17 and 9, respectively, can be calculated as follows:

$$\left(\tau'_{\max}\right)_{FF} = 1.29 \times 17,000 = 22,000 \text{ psi}$$

$$\left(\tau'_{\max}\right)_{FF} = 1.29 \times 22,700 = 29,400 \text{ psi}$$

The surprisingly high initial stresses indicated by the preceding indirect analysis suggested the advisability of making direct measurements during assembly of a typical joint. Such tests have been made. (See reference 3.) Before assembly, SR-4 strain gages were cemented to the gusset between rivet holes across section FF. The gusset was then riveted to the columns and the gage resistance again measured. The axial stress produced in the gusset by assembly of the joint was found to be approximately 25,000 psi.

If the reasonable assumption is made that the initial stresses are distributed similarly to the load-applied stresses, the result given in reference 3 would indicate an initial maximum shear stress of approximately 21,900 psi. (In support of such an assumption is the fact that in a few tests, in which rivets became loose during the progress of the test, the ratio of maximum principal stress to shear stress remained the same throughout the run.) This is of the same order of magnitude predicted by the fatigue test results.

It should be noted that, according to this analysis, failures across section EE should occur after a greater number of fatigue cycles than failure across section FF for the same load range. The result obtained does not in general bear this out, and in at least one case the discrepancy is too large to be attributed to the normal scatter of fatigue data. However, there can be little question that initial stress in the gusset is dominant in determining fatigue life in the low and intermediate range of load cycles.

Heat-Treated Alloy-Steel Gussets

In the second phase of this testing program, heat-treated alloy-steel gussets were used in place of the 24S-T gussets. Tubes, rivets, rivet spacing, and fabrication procedure were the same as for the 24S-T riveted gussets. (See table 2 and fig. 3.) The gussets were

saw-cut and were reduced in cross-sectional area consistently with the increase in yield strength and ultimate strength of the heat-treated alloy steel, as compared to the same properties of the 24S-T aluminum alloy. Here again, edge finish was found to have no effect on fatigue life. All fatigue cracks, with the exception of two which were undetermined, originated at rivet holes on section EE. (See fig. 8.)

Initial stresses due to riveting apparently had no effect on fatigue life in the load ranges investigated, as no failures occurred across the gross section FF. On noting that the maximum stress P/A in these gussets during load cycle 1 is greater than that in the 24S-T gussets during load cycle 5, this result is to be expected if initial stresses of the same order of magnitude in both types of gusset are assumed.

Strain-gage readings were taken on all specimens run below load schedule 4. These readings were taken as a matter of routine and had no significance with regard to interpretation of the data and are, therefore, omitted. The loosening of rivets during dynamic loading was evident in all tests. Under heavy loads (loads 4 to 7) a majority of the rivets became loose and under lighter loads an average of about three or four rivets was loosened. Reference to figure 6 shows that the fatigue life of alloy-steel gussets is less than that of the 24S-T gussets at all load conditions.

Spot-Welded 24S-T Alclad Columns and Gussets

The spot-welded gusset joints were revised in several details of construction. (See table 2 and fig. 3.) The columns were pressed to shape in halves, reinforced at the ends for bolting and flanged at the center section so that the gussets could be spot-welded in place, and the two halves were spot-welded together by means of the flanges. The reinforced ends were jig-drilled so that over-all dimensions remained the same, and the same end brackets were used as for all the previous tests. Table 3 gives the essential load and test-result data for this group of spot-welded specimens. The results are plotted in figure 6.

The first test in this series, test 34 (table 3), was fitted with metaelectric gages on the outer surface of the gussets on section FF and showed an average tensile stress of 31 percent as compared with the uniform stress P/A for that section. Furthermore, it was found that, while adding and removing the static load for purposes of verification, the average-stress readings increased on this section with each repetition of the load.

Test 35 gave essentially the same results as test 34, the average tensile stress on section FF being somewhat lower, or 22 percent of the uniform stress P/A . Dynamically, 43 percent was recorded.

Specimen 36 was revised by milling the column flanges away at the center gap and by inserting a spacer to prevent the gussets from drawing in or "breathing" under dynamic loading. In static tests specimen 36 showed 16 percent of the stress P/A without the spacer inserted and 62 percent with the spacer inserted. In dynamic loading the average tensile stress showed 90 percent of the uniform stress P/A with the spacer in place. The fatigue life of the joint was not materially changed with the spacer inserted, as the fatigue failure was forced to another critical section (section AA) and a crack developed in the column member. Figure 9 shows typical failures for spot-welded joints; the failures had their origin at the spot welds on section EE.

Specimen 48 was tested by filling the column with plaster of paris for distance equal and adjacent to the gussets. On section FF at the opening in the column the plaster of paris was cut into two parts to prevent a transfer of the load through the plaster of paris. In this manner a substantial filler was provided in the column to prevent the "breathing action" of the gusset plates upon loading the column in tension. Based upon average values of readings taken of section FF, the following comparison may be presented in tabular form:

Condition of specimen	Ratio of stress to P/A (percent)	
	Static	Dynamic
Without backing	21	43
With wedging	62	90
With plaster of paris	75	71

Figure 10 is given to illustrate the apparent action at section FF over the joint of the column. Micrometer readings from gusset face to gusset face before and after static loading to 4000 pounds are plotted in figure 10(a). If the plot of the face is extended to section FF, it is shown that each gusset plate draws in 0.013 inch, while at the same time micrometer readings show 0.016 inch actual deflection on section FF. Figure 10(b) shows the section to scale longitudinally but magnified vertically. Figure 10(c) shows the distortion of gusset and column under a 4000-pound load.

All failures in spot-welded gussets originated at the periphery of the spot weld on section EE or AA. (See fig. 9.) In two cases failure occurred simultaneously across sections EE and AA. In one case, in which a wedge was used to minimize bending, failure occurred across section AA. All other failures were on section EE.

The results reaffirm the fact that spot welds, because of the high stress concentration inherent in their geometry and of the metal structure in the kernel of the weld, are inferior to riveted connections in their fatigue characteristics.

CONCLUSIONS

Data obtained from tests on gusseted joints to determine the effect of gusset edge finish on fatigue life and to compare riveted with spot-welded assemblies lead to the following conclusions:

1. For the simple type of gusseted joint tested, edge finish of the gussets (whether saw-cut or stamped) had no effect on fatigue life.

2. For a given cross-sectional area in a gusset, the narrower gusset seemed to give longer fatigue life than wider gussets under the same load conditions.

3. In the 24S-T riveted joint (and possibly in the alloy-steel assembly) two factors appeared dominant in determining fatigue life of the gusset:

- (a) When the load cycle is such that the highest average stress across the gross section is less than about 23,000 psi, initial stresses in the gusset limited its fatigue life, and failure occurred across the gross section.

- (b) In the higher stress range, stress concentration at the rivet holes limited fatigue life, and failure occurred across a net section.

4. In the spot-welded assemblies, the potential fatigue life of the material was severely reduced by the stress concentration at the spot welds in the extreme positions.

5. The riveted gusset joints gave better performance under cyclic loading than the spot-welded joints, and of the riveted assemblies, those with the 24S-T aluminum gussets had longer fatigue life than those with the alloy-steel gussets under the same load

conditions. The three types of joint tested failed under approximately the same load in static tests.

State College of Washington
Pullman, Washington
March 20, 1947

APPENDIX

PHOTOELASTIC STUDY OF GUSSET PLATE

The model of the 24S-T gusset assembly for the photoelastic study was made of a clear plastic material. The gussets were made to full scale, and flat stock having the same effective cross section as the two riveted sides of the 24S-T column was used as column members to transmit the applied loads to the gussets through the rivets. Plastic dowels, reinforced with 0.1-inch-diameter brass cores, were machined to give a press fit in the rivet holes of the columns and gussets and were used in place of rivets.

The "frozen stress pattern" technique (reference 4) was used, since it permits the observation of the stress distribution in the component parts of the model separately after removal of external loads. The axial load applied to the model at 110° C was 8.25 pounds. The material fringe value in tension per inch of thickness was 3.22 psi. (See references 5, 6, and 7.)

The results of the photoelastic method made it possible to obtain a more complete "picture" of the stress relations existing across the gusset plate than was given by the use of a necessarily limited number of resistant gages. Figure 11 shows these stress relations on both section EE and section FF.

REFERENCES

1. Wilkinson, C. A.: Fatigue Study of Gusseted Joints. Rep. No. D-4005, Boeing Aircraft Co., 1942.
2. Anon.: SR-4 Strain Gage. Bull. 164, Baldwin Southwark, Div. of the Baldwin Locomotive Works, 1942.
3. Martin, H. C.: Stresses in Gussets as a Result of Riveting. Test Rep. No. T-21492, Boeing Aircraft Co., 1943.
4. Hetenyi, M.: Application of Hardening Resins in Three Dimensional Photoelasticity. Jour. Appl. Phys., no. 5, vol. 10, May 1939, p. 295.
5. Coker, E. G., and Filon, L. N. G.: A Treatise on Photo-Elasticity. The Univ. Press (Cambridge), 1931.
6. Frocht, Max Mark: Photoelasticity. J. Wiley & Sons, Inc. (New York), 1941.
7. Fried, Bernard, and Weller, Royal: Photoelastic Analysis of Two- and Three-Dimensional Stress Systems. The Eng. Experiment Station Bull. No. 106, Ohio State Univ. Studies Eng. Series Bull., vol. IX, no. 4, July 1940.

TABLE 1.- LOAD CYCLES FOR TESTS

[Positive values, tension; negative values, compression]

Load cycle	Load factor (maximum and minimum, respectively)	Ultimate design load (percent)	Machine- applied load	Stress on EE section	Stress range
	1	20	4,000	10,800	
1	$1\frac{1}{3}$	26.7	5,340	14,400	7,200
	$\frac{2}{3}$	13.3	2,660	7,200	
2	$1\frac{2}{3}$	33.3	6,660	17,900	14,300
	$\frac{1}{3}$	6.6	1,320	3,600	
3	2	40	8,000	21,500	21,500
	0	0	0	0	
4	$2\frac{1}{3}$	46.7	9,340	25,100	27,900
	$-\frac{1}{3}$	-6.6	-1,320	-2,800	
5	$2\frac{2}{3}$	53.3	10,660	28,700	34,400
	$-\frac{2}{3}$	-13.3	-2,660	-5,700	
6	3	60	12,000	32,300	40,900
	-1	-20	-4,000	-8,600	
7	$3\frac{1}{3}$	66.7	13,340	35,900	47,400
	$-1\frac{1}{3}$	-26.7	-5,340	-11,500	

TABLE 2.- SPECIFICATIONS OF TEST SPECIMENS

Specimen	Gusset material	Column material	Width of gusset (in.)	Thickness of gusset (in.)	Gross area of gusset (sq in.)	Area of column (sq in.)	Rivets	Gussets
Riveted								
1 to 10 12, 15, 18, 46	24S-T ¹	24S-T ²	2.56	0.091	0.233	1.149	24S-T	Stamped
11	24S-T	24S-T ³	2	.125	.250	1.36	24S-T	Saw-cut
13	24S-T	24S-T	1.55	.188	.291	1.36	24S-T	Saw-cut
14, 16 17, 19, 20	24S-T	24S-T	2.56	.091	.233	1.36	24S-T	Stamped
21 to 33	Alloy steel ⁴	24S-T	1.5	.062	.0947	1.36	24S-T	Saw-cut
Spot-welded								
34 to 48	24S-T ⁵	24S-T ⁵	2.56 ⁵	0.091	0.233	Not determined	Spot welds	Sheared

¹QQ-3-355.²QQ-3-355.³Army - 10235.⁴X4130-AN-QQ-S685. Heat-treated; yield strength, 180,000 psi.⁵Alclad 24S-T. Both gusset and column cut from 0.091-inch sheet.

TABLE 3.- SUMMARY OF TEST RESULTS

Specimen	Load cycle	Minimum load (lb)	Minimum stress on section EE, P/A (psi)	Maximum load (lb)	Maximum stress on section EE, P/A (psi)	Load range (lb)	Stress range (psi)	Cycles to failure	Remarks
24S-T riveted gussets									
1	1	2660	7200	5340	14,400	2,680	7,200	10,000,000	No failure ^a
2	2	1320	3600	6660	17,900	5,340	14,300	740,000	Failure progressed from center to edges on section FF
3	2	1480	3970	6520	17,500	5,040	13,630	588,000	Center to edge on section FF on one gusset
19	3	0	0	8000	21,500	8,000	21,500	166,800	Center to edge on section EE
4	3	215	580	7785	20,900	7,570	20,320	164,000	Center to edge on section FF on one gusset
18	3	0	0	8000	21,500	8,000	21,500	274,000	Center to edge on section EE
5	3	0	0	8000	21,500	8,000	21,500	452,000	Incipient crack in center of one gusset
17	3	0	0	8000	21,500	8,000	21,500	199,200	Center to edge on sections EE and FF
6	4	-1320	-2800	9340	25,100	10,660	27,900	228,000	Center to edge on section FF on one gusset

^aSee figures 6, 7, and 8 for types of failure.

TABLE 3 - SUMMARY OF TEST RESULTS - Continued

Specimen	Load cycle	Minimum load (lb)	Minimum stress on section EE, P/A (psi)	Maximum load (lb)	Maximum stress on section EE, P/A (psi)	Load range (lb)	Stress range (psi)	Cycles to failure	Remarks
24S-T riveted gussets									
7	4	-1320	-2,800	9,340	25,100	10,660	27,900	53,600	Center to edge on section EE on one gusset
8	4	-1320	-2,800	9,340	25,100	10,660	27,900	122,400	Incipient crack in center of gusset
20	4	-1320	-2,800	9,340	25,100	10,660	27,900	61,600	Center to edge on section EE on one gusset
9	5	-2660	-5,700	10,660	28,700	13,320	34,400	51,600	Center to edge; moved from FF to EE
10	5	-2660	-5,700	10,660	28,700	13,320	34,400	39,600	Center to edge on section FF
15	6	-4000	-8,600	12,000	32,300	16,000	40,900	24,000	Center to edges; both gussets on section EE
12	7	-5340	-11,500	13,340	35,900	18,680	47,400	6,800	Center to edges on section EE
^b 11	3	0	0	8,000	21,500	8,000	21,500	464,000	Rivet hole to edges on section EE
^c 13	3	0	0	8,000	20,500	8,000	20,500	648,000	Center between rivets progressed to edges on section EE
46	Static	-----	-----	24,190	65,000	-----	-----	-----	Center to edges on section EE

^b24S-T aluminum-alloy 2- by 0.125-inch gusset with saw-cut edges. Net area = $2 \times 0.186 = 0.372$ square inch.

^c24S-T aluminum-alloy 1.5- by 0.188-inch gusset with saw-cut edges. Net area = $2 \times 0.195 = 0.390$ square inch.



TABLE 3 - SUMMARY OF TEST RESULTS - Continued

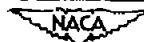
Specimen	Load cycle	Minimum load (lb)	Minimum stress on section EE, P/A (psi)	Maximum load (lb)	Maximum stress on section EE, P/A (psi)	Load range (lb)	Stress range (psi)	Cycles to failure	Remarks
Steel-alloy gussets									
21	7	-5340	-39,800	13,340	99,600	18,680	139,400	6,000	Failure from center to edge on section EE (one gusset)
22	7	-5340	-39,800	13,340	99,600	18,680	139,400	6,200	Center to edge on section EE (both gussets)
23	6	-4000	-29,850	12,000	89,600	16,000	119,450	12,000	Center to edge on section EE (both gussets)
24	6	-4000	-29,850	12,000	89,600	16,000	119,450	7,400	Progression undetermined; section EE (both gussets)
25	5	-2660	-19,850	10,660	79,600	13,320	99,450	12,200	Center to edge on section EE (one gusset)
26	5	-2660	-19,850	10,660	79,600	13,320	99,450	16,800	Center to edge on section EE (one gusset)
27	4	-1320	-9,850	9,340	69,700	10,660	79,550	25,400	Center to edge on section EE (one gusset)
28	4	-1320	-9,850	9,340	69,700	10,660	79,550	28,800	Center to edge on section EE (one gusset)
29	3	0	0	8,000	59,700	8,000	59,700	100,400	Progression unknown; section EE (one gusset)
30	3	0	0	8,000	59,700	8,000	59,700	85,800	Center to edge on section EE (one gusset)
31	2	1320	9,850	6,660	49,700	5,340	39,850	257,200	Rivet hole to edge; section EE
32	1	2660	19,850	5,340	39,800	2,680	19,950	6,000,000	Not run to failure
33	Static	-----	-----	28,400	210,000	-----	-----	-----	Center to edges on section EE



TABLE 3 - SUMMARY OF TEST RESULTS - Continued

Specimen	Load cycle	Minimum load (lb)	Minimum stress on section EE, P/A (psi)	Maximum load (lb)	Maximum stress on section EE, P/A (psi)	Load range (lb)	Stress range (psi)	Cycles to failure	Remarks
Spot-welded joints									
34	2	1320	2820	6,660	14,300	5,340	11,480	53,400	Center to edges; section EE through edge of welds in gusset
35	2	1320	2820	6,660	14,300	5,340	11,480	80,200	Incipient failure center to edges; sections EE and AA in gusset
36	2	1320	2680	6,660	19,300	5,340	11,480	68,400	Center to edge in column on section AA
37	1	2660	5700	5,340	11,450	2,680	5,750	938,800	Center to edge through edge of spot welds; section EE
38	4	1320	2820	9,340	20,000	10,660	22,820	5,600	Center toward edges and through edges of spot welds on section EE
39	4	1320	2820	9,340	20,000	10,660	22,820	23,600	Center to edges through edge of spot welds; section EE
40	3	0	0	8,000	17,200	8,000	17,200	44,800	Incipient failure at edge of spot welds; section EE
41	3	0	0	8,000	17,200	8,000	17,200	41,600	Incipient failure at edge of spot welds; section EE
42	5	-2660	-5700	10,660	22,900	13,320	28,400	7,200	Incipient failure at edge of spot welds; section EE
43	5	-2660	-5700	10,660	22,900	13,320	28,400	4,000	Center to edges and through edges of spot welds on section EE
45	2	1320	2820	6,660	14,300	5,340	11,480	24,190	Incipient failure at edges of spot welds; section EE
47	Static	-----	-----	26,210	70,500	-----	-----	-----	Center toward edges and through edges of spot welds
48	2	1320	2820	6,600	14,300	5,340	11,480	121,200	Section EE; through edge of spot welds
49	6	-4000	-8600	12,000	25,700	16,000	34,300	4,800	Section EE on gusset and section AA on column

^dGages located inside column as well as outside.



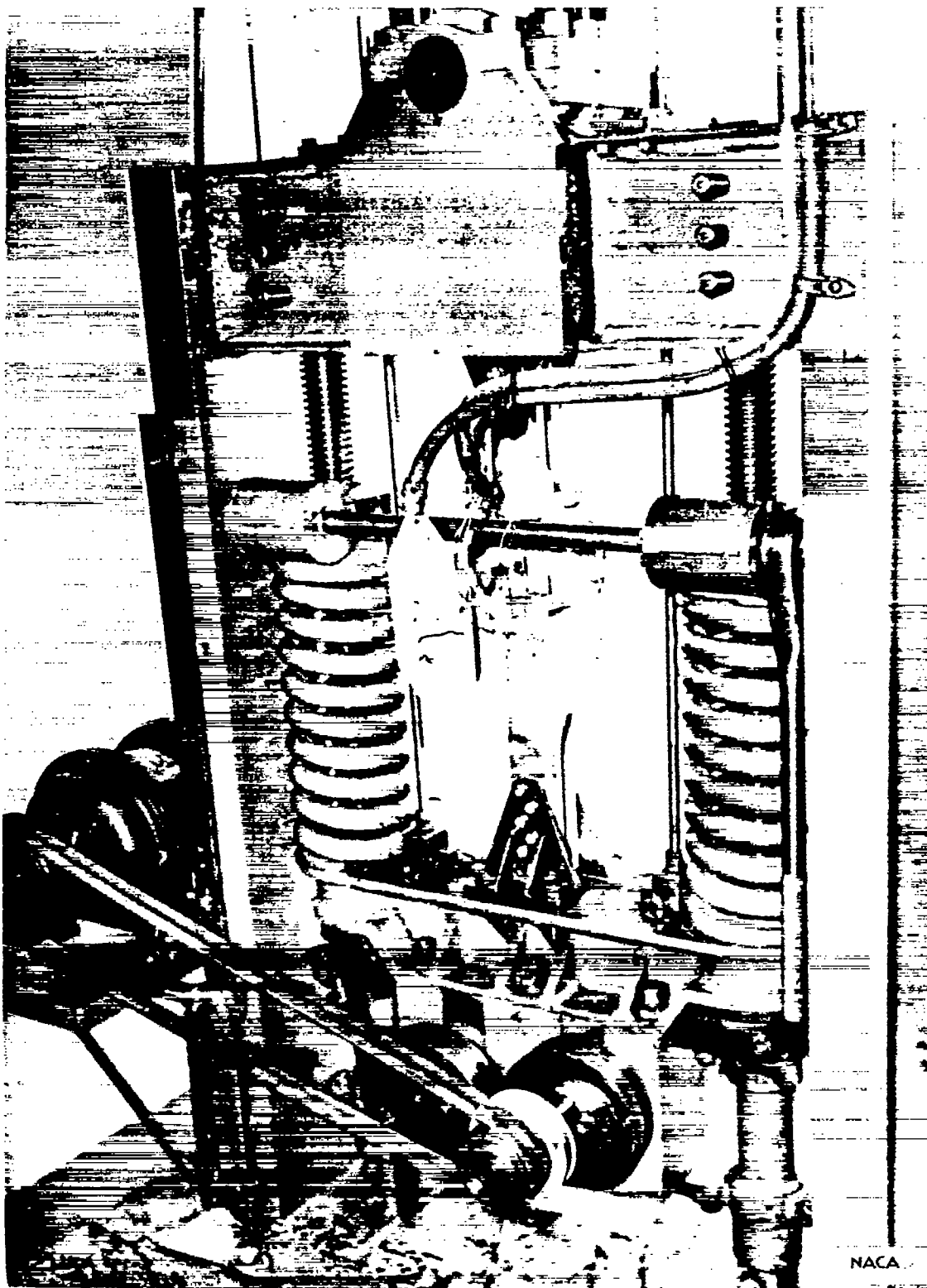


Figure 1.- Fatigue testing machine with test specimen in place.

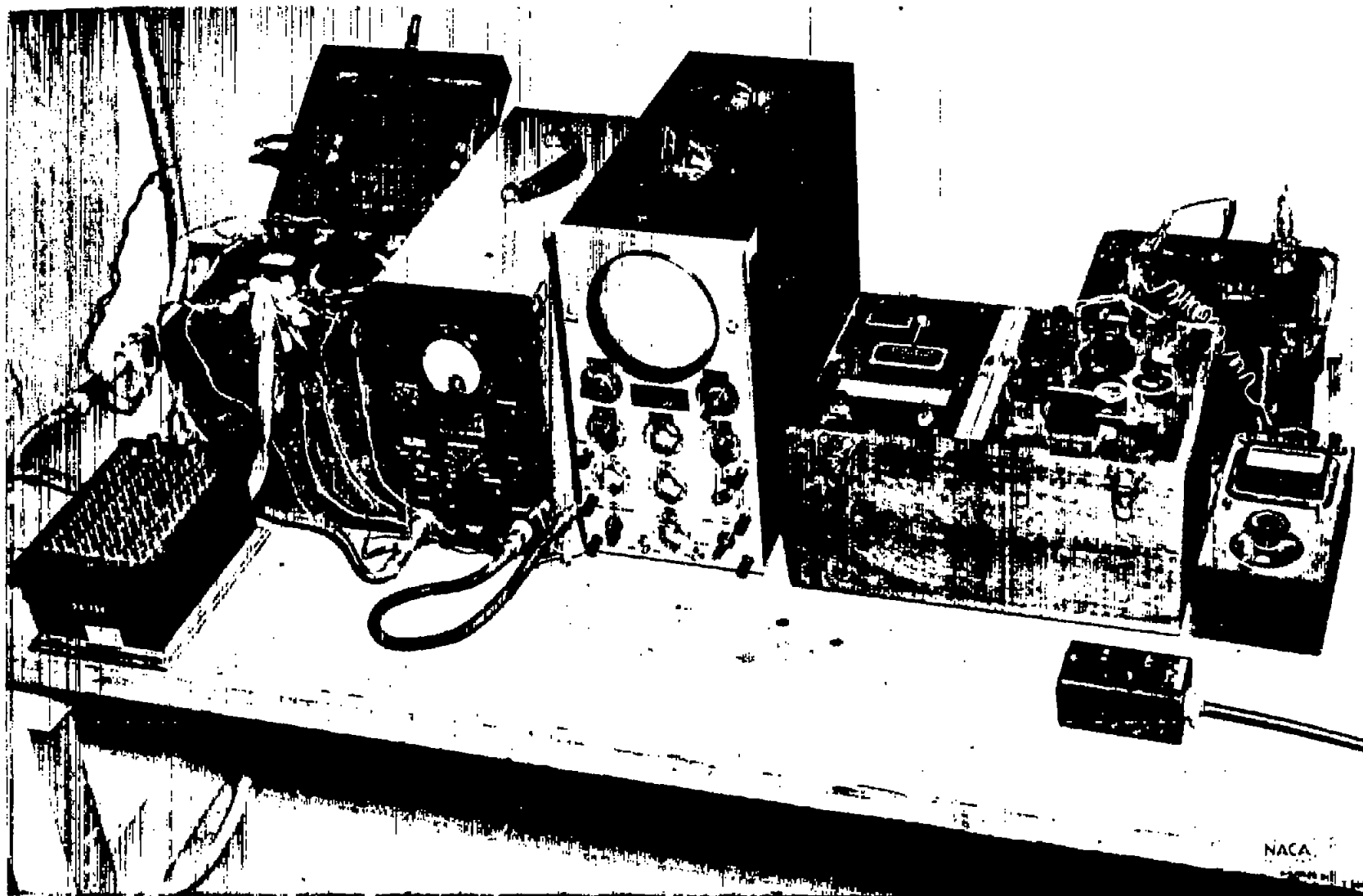


Figure 2.- Strain measuring equipment. Driving and calibrating units in box shown at left-hand side.

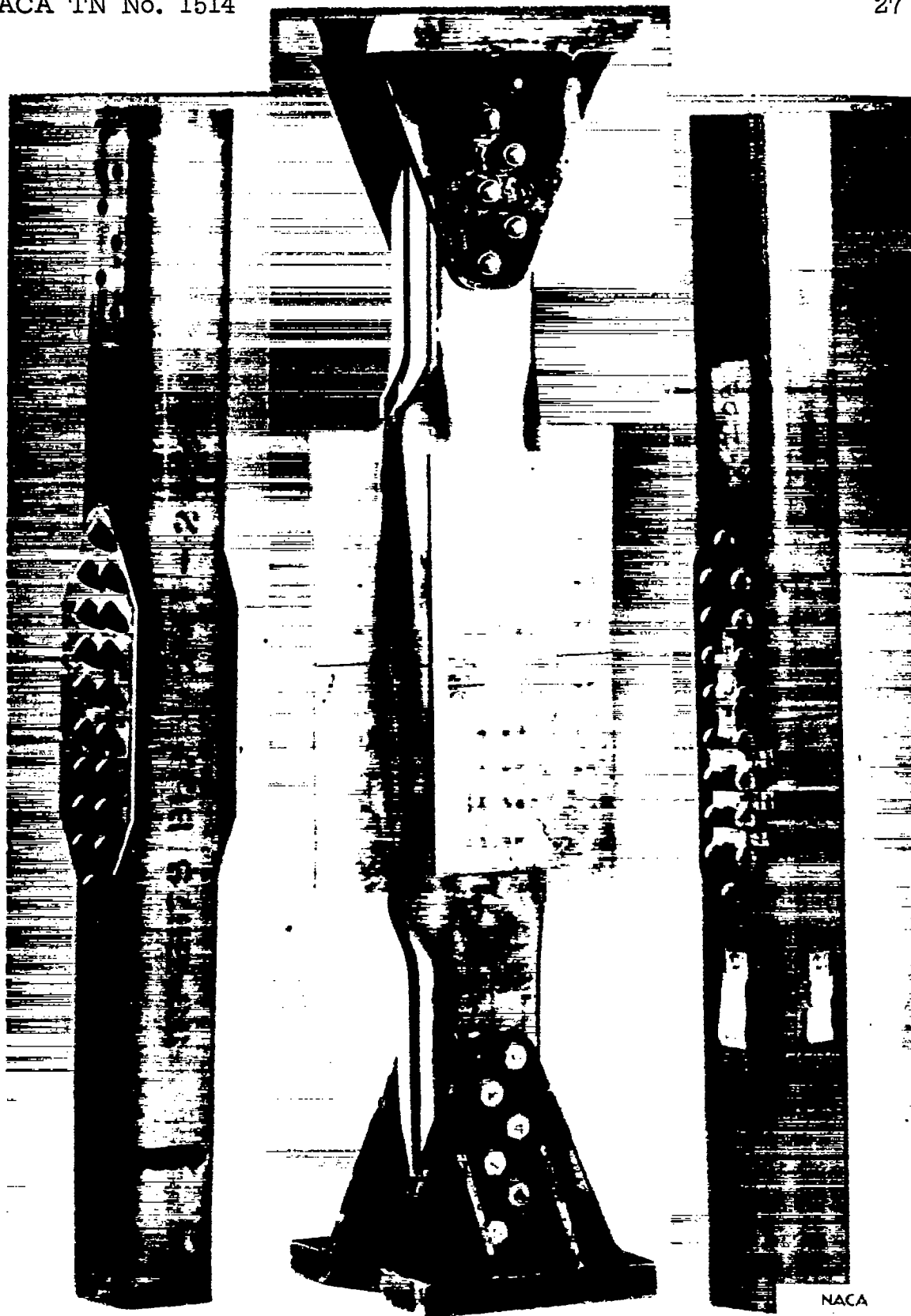


Figure 3.- Three types of specimen tested.

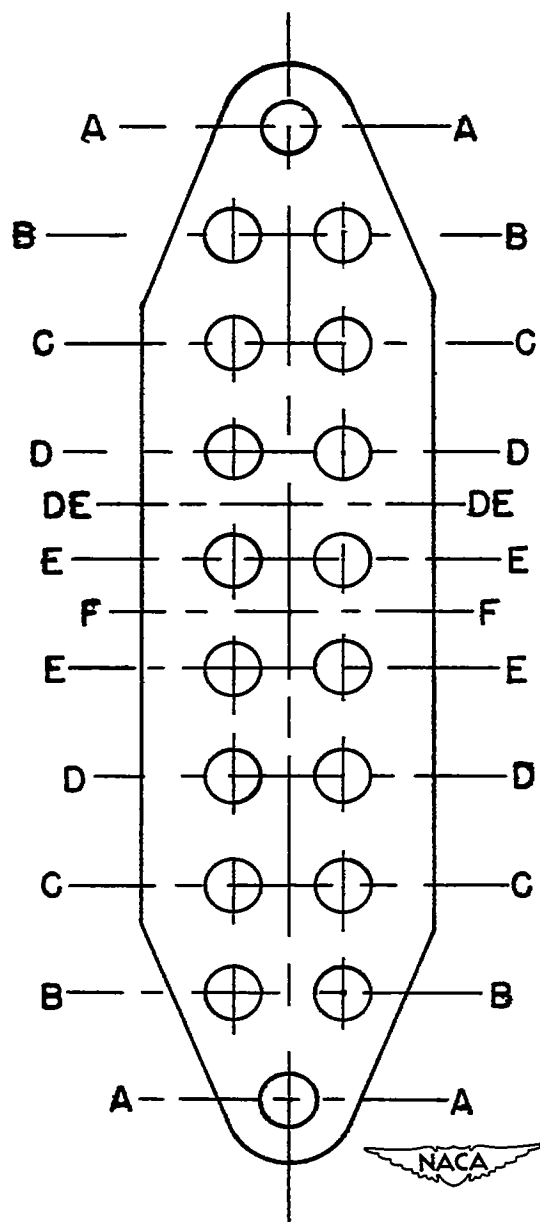


Figure 4.- Diagram showing sections of specimens.

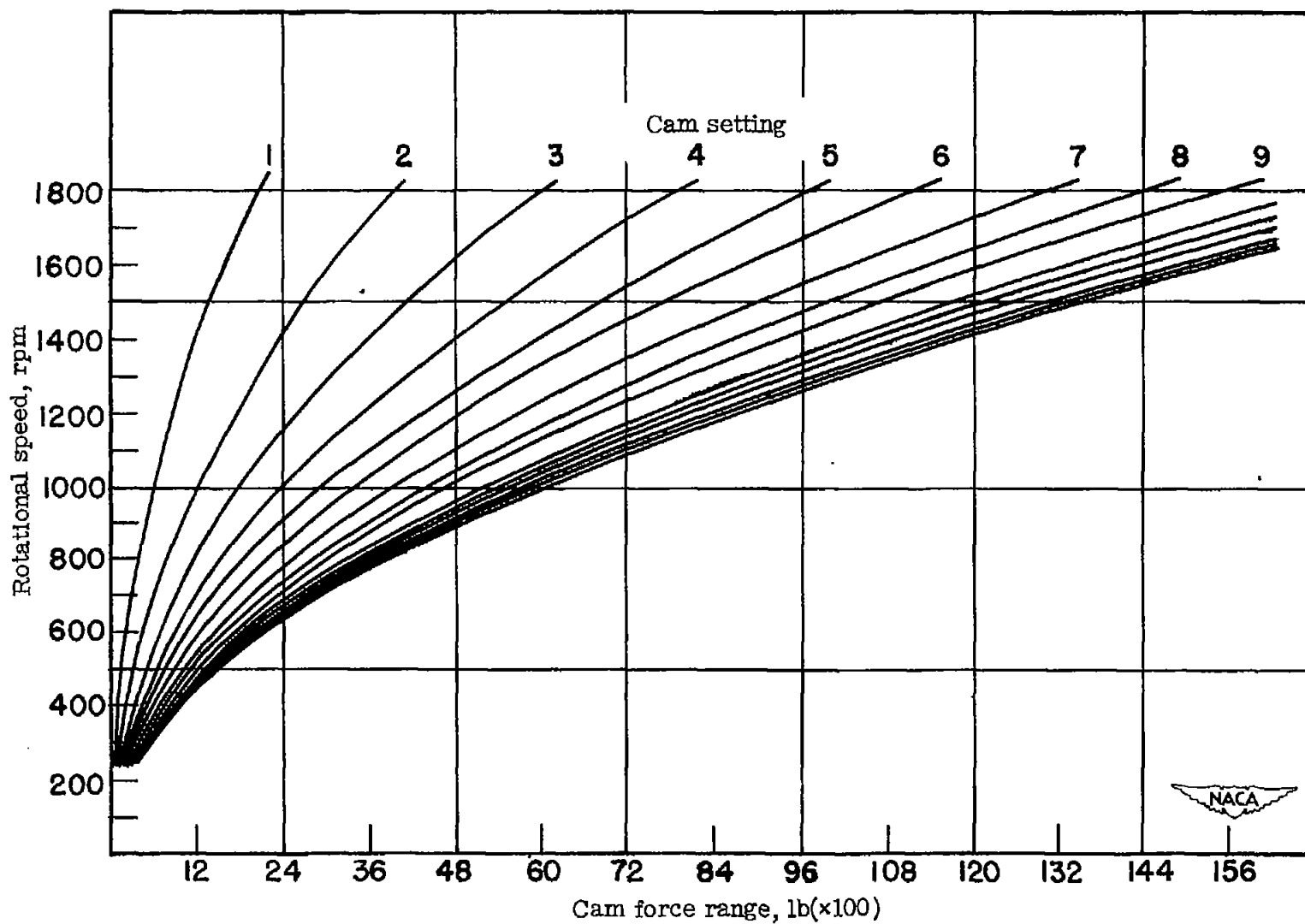


Figure 5.- Dynamic-force diagram for testing machine.

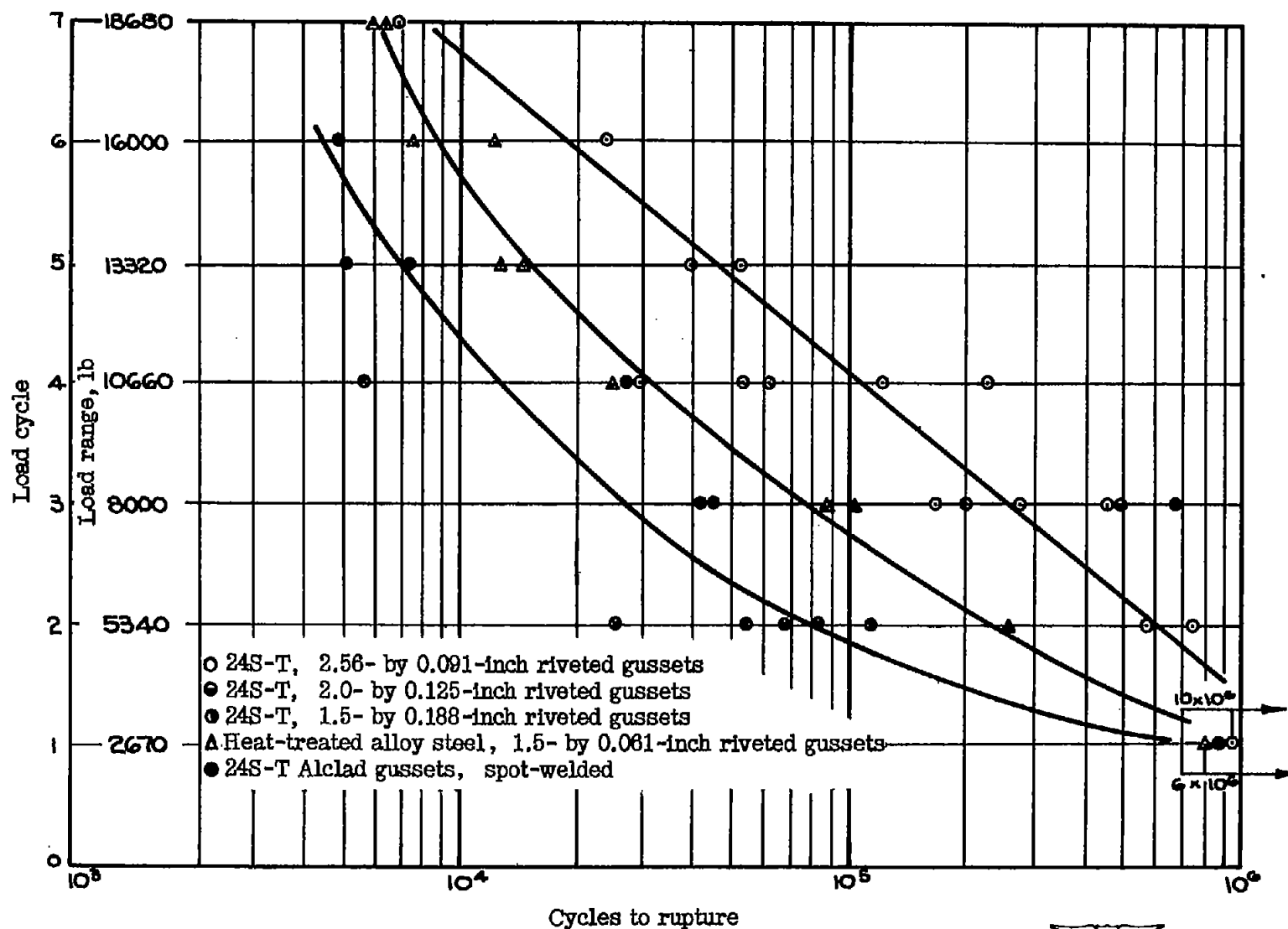


Figure 6.- Fatigue test results.



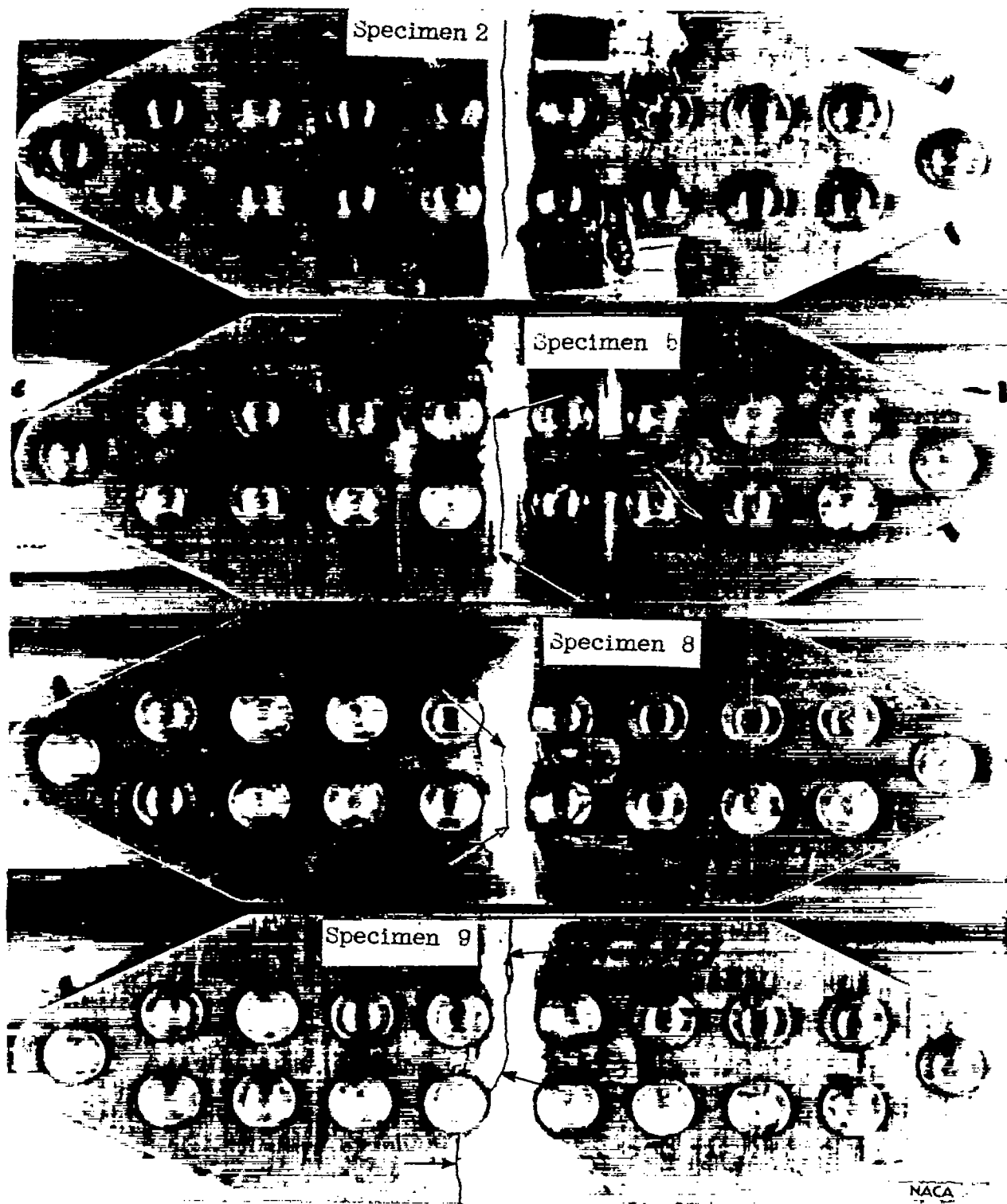


Figure 7.- Progression of fatigue cracks.

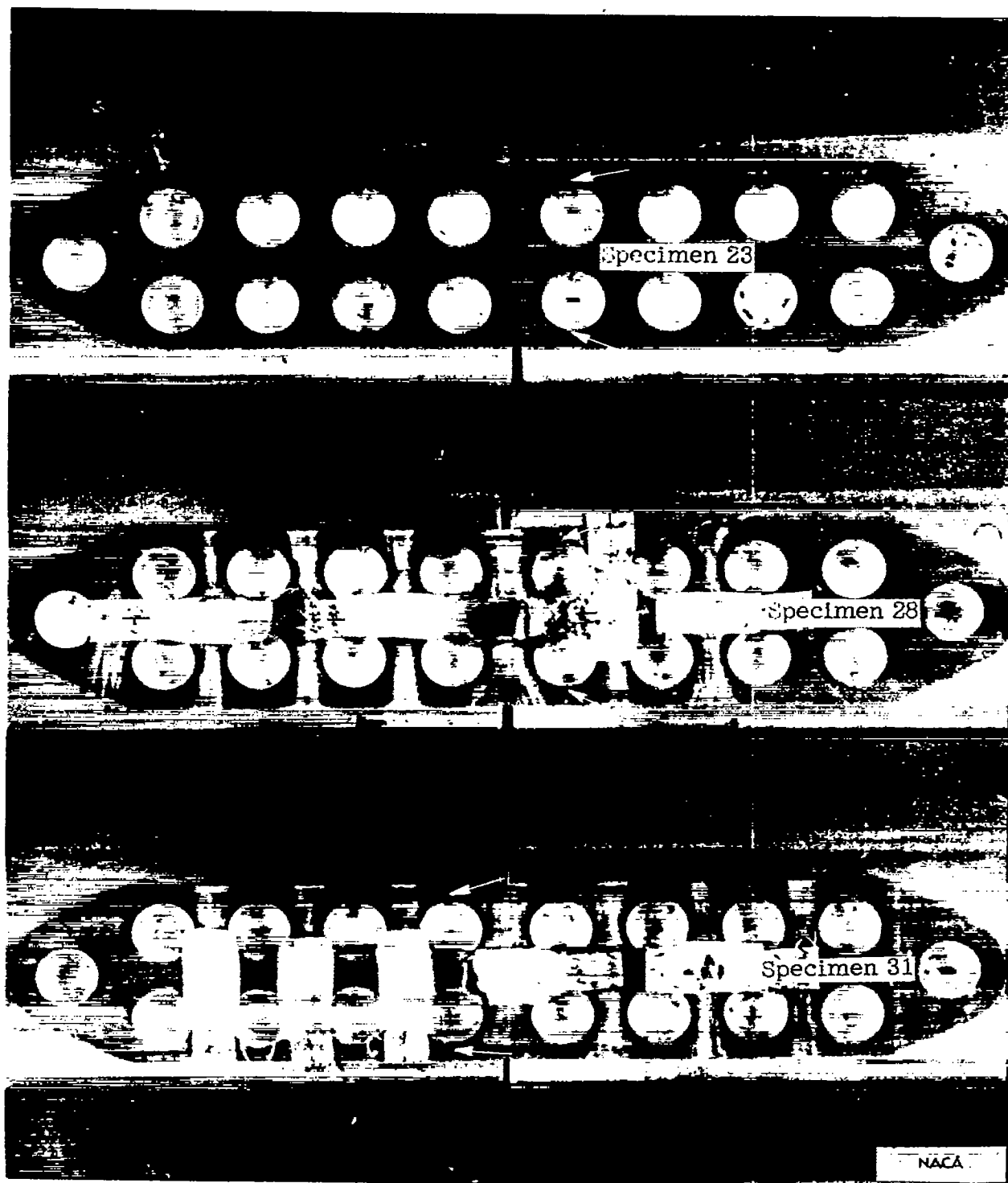
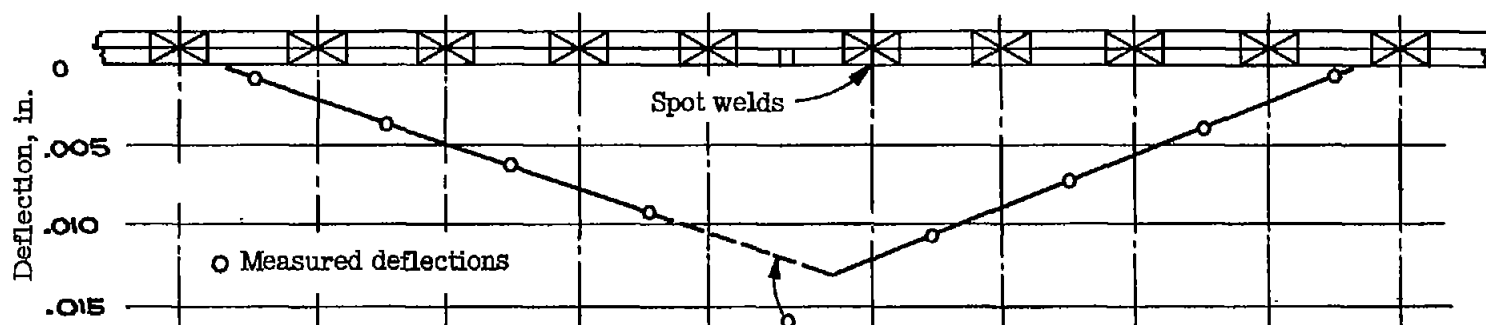


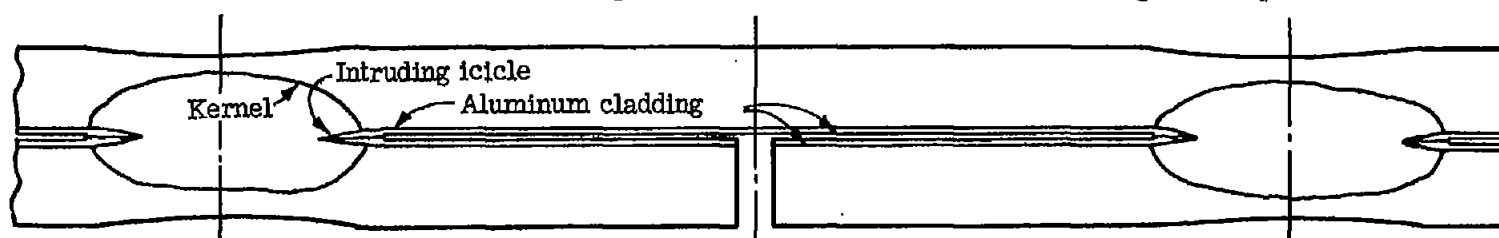
Figure 8.- Typical failure originating at rivet holes.



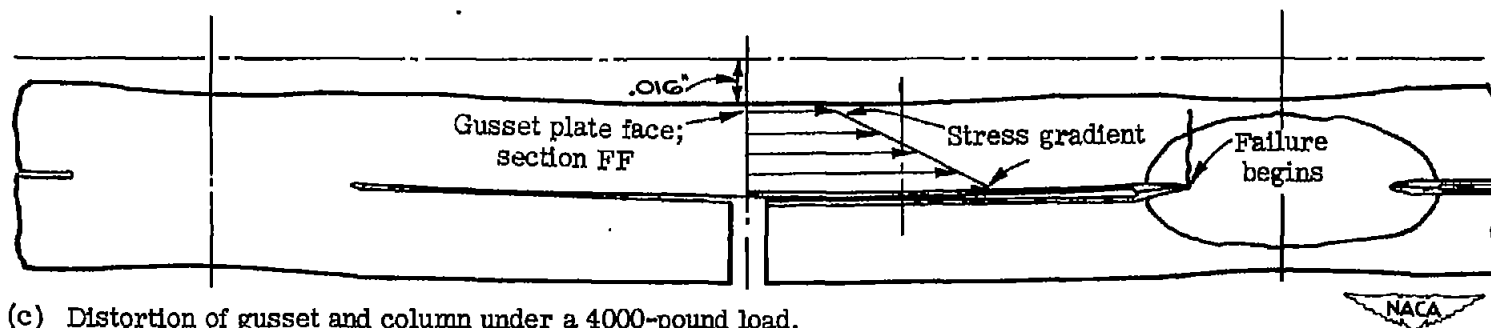
Figure 9.- Typical failures for spot-welded joints.



(a) Micrometer readings from gusset face to gusset face before and after static loading to 4000 pounds.



(b) Section to scale longitudinally but magnified vertically. Without load.



(c) Distortion of gusset and column under a 4000-pound load.

Figure 10.- Apparent joint action for spot-welded joints.

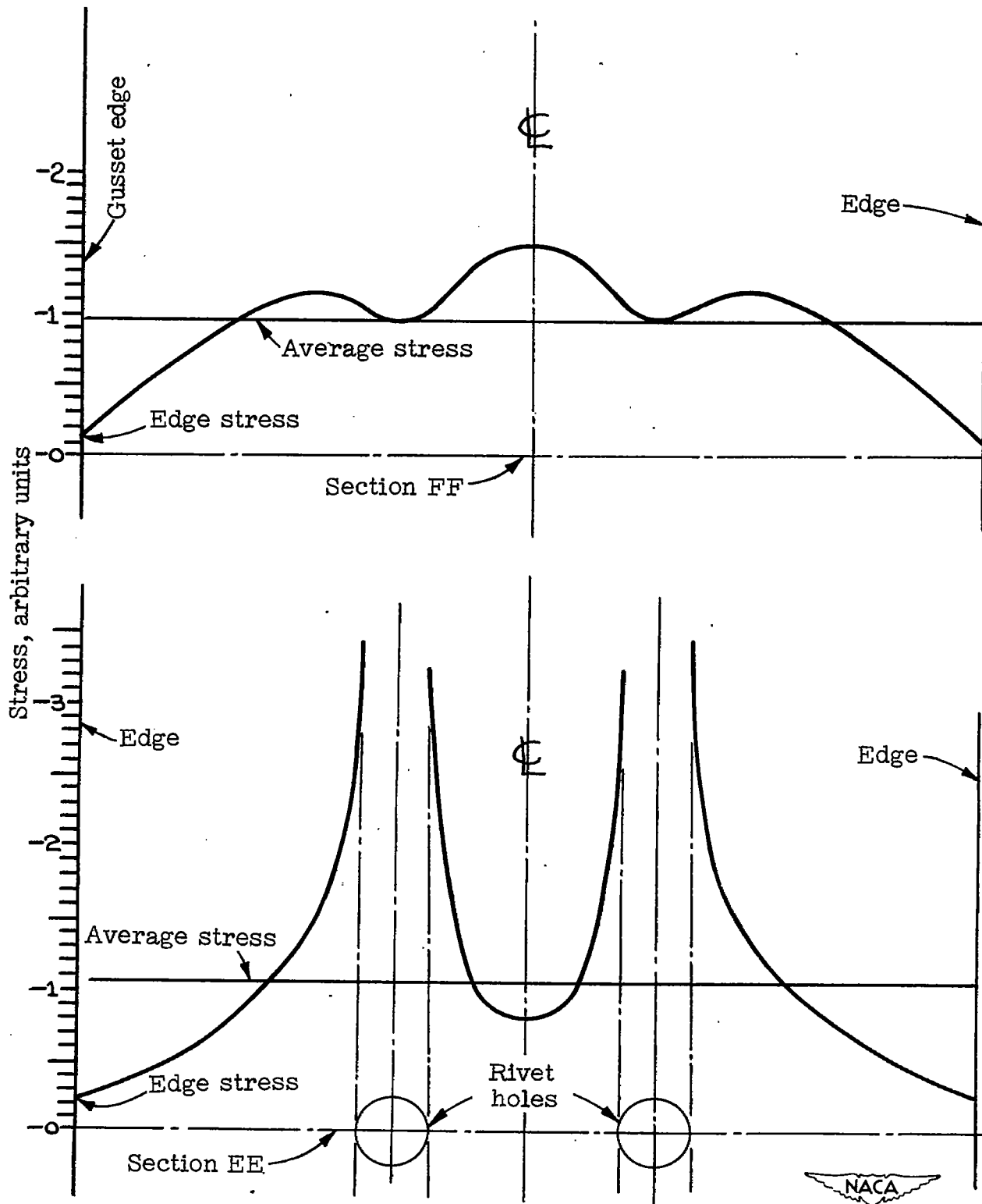


Figure 11.- Variation of stress with width of gusset plate.
Photoelastic method.